

# Whispering Gallery Modes in Bottle Microresonators

Michalis N. Zervas, G. Senthil Murugan and James S. Wilkinson

*Optoelectronics Research Centre, University of Southampton, Southampton SO17 1BJ, United Kingdom.*

## ABSTRACT

Selective excitation of an extended range of whispering gallery modes (WGM) supported by bottle microresonators fabricated on a short section of optical fiber is demonstrated experimentally and discussed theoretically. Decrease of the observed Q factors, as the excitation point moves away from the bottle centre, are associated with increased mode leakage. Compared to standard-fiber cylindrical resonators, the bottle microresonator results in a 35x increase of the observed Q factor.

**Keywords:** Microresonators, bottle resonators, optical filters, optical delay lines, photonic harmonic oscillators.

## 1. INTRODUCTION

Optical whispering-gallery mode (WGM) microresonators, with different geometries and associated unique characteristics, have attracted considerable research interest over the years. Their main attribute is the ability to confine light spatially and temporally, resulting in small mode volumes and large optical quality factors (Q), yielding high optical intensities and long photon lifetimes. The combined small mode volume and high Q make them attractive for applications including compact optical elements, narrow linewidth microlasers, biosensors, all-optical switching and cavity quantum electro-dynamics (CQED) [1-5]. Among them, micro-ring/-disc resonators are convenient for device integration [1]. However, the Q's of such resonators are limited by the surface roughness introduced by the fabrication techniques, such as photolithography and dry etching. On the other hand, glass microsphere resonators fabricated by melt/re-melt processing may possess record-high Q factors ( $\approx 10^{10}$ ) [6]. Another widely used and studied WGM microresonator with remarkable performance is the microtoroid with  $Q \approx 10^8$  [7].

The whispering gallery mode bottle microresonator was proposed recently and has been studied theoretically [8-10]. Bottle resonators are highly oblate resonators and sustain non-degenerate WGMs that exhibit two well-separated spatial regions with enhanced field strength, corresponding to modal turning points. The free spectral range (FSR) of such resonators is predicted to be about one order of magnitude smaller than that of microsphere resonators of equal diameter [9]. The reduced FSR is particularly useful when tuning of a high-Q WGM is required to match atomic transition lines in experiments such as CQED [9].

So far, bottle microresonators have been fabricated primarily by "heat-and-pull" techniques, using modified fibre taper rigs [11-13]. A CO<sub>2</sub> laser has been used to heat the fibre locally while it is pulled in a controlled fashion. Early attempts [11,12] resulted, however, in rather poor resonator qualities and measured Q factors of about 3000-4000 [11]. In order to improve the bottle resonator performance, much more advanced fibre taper rigs have been recently employed [13].

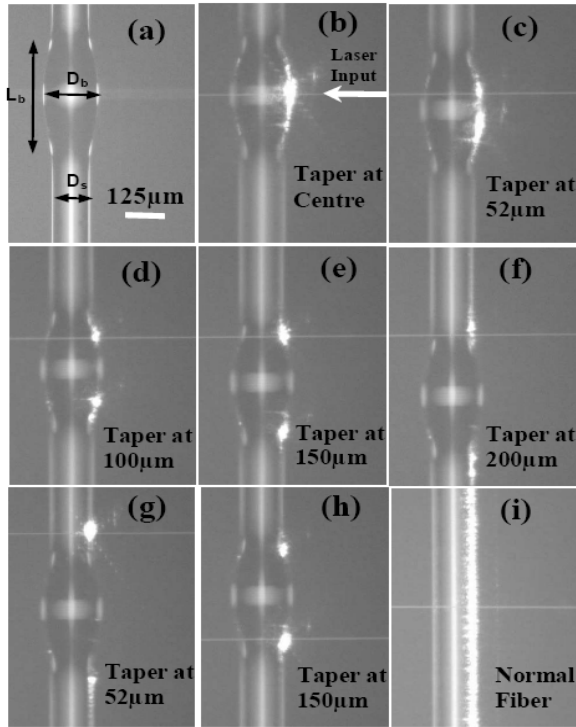
We have fabricated fiber WGM bottle microresonators from short sections of optical fiber by an alternative simple and versatile "soften-and-compress" technique using a standard fusion splicer to soften the fiber locally [14]. In this paper, we present clear experimental evidence of the turning points and the associated intensity maxima of the bottle resonator modes. In addition, we show transmission spectral characteristics when the bottle is evanescently excited at different points along its length.

## 2. EXPERIMENTAL CHARACTERIZATION

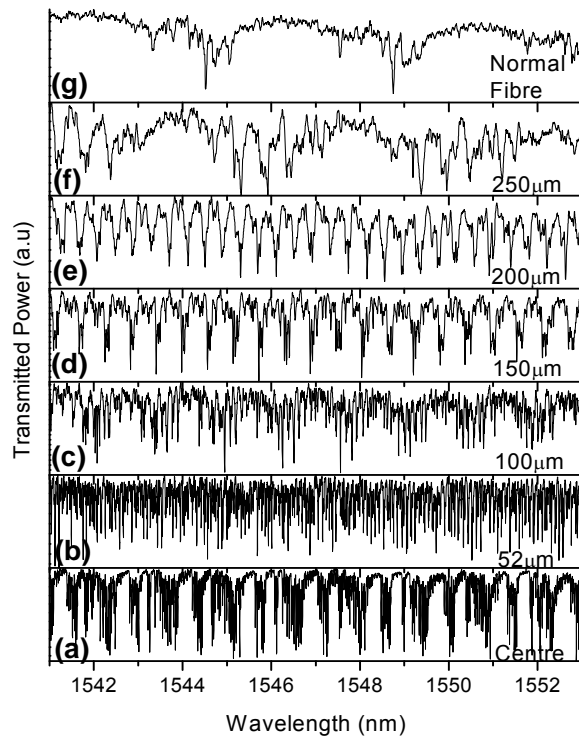
The "soften-and-compress" microbottle fabrication technique has been outlined in Ref. [14]. The procedure results in a robust, double-neck bottle fiber microresonator with neck-to-neck distance  $L_b$ , bottle diameter  $D_b$  and stem diameter  $D_s$ . The detailed "bottle" shape is also an important parameter in defining the spectral characteristics and optical properties of the resonator, and it is defined by the softening temperature profile and applied compression. A tapered fiber with diameter of about 2μm was used to couple light into and out of the bottle resonator. Micro-positioning stages were used to place the tapered fiber on top of, and in close proximity to, the resonator, as close to right angles to the fiber axis as obtainable by inspection. A narrow linewidth, tunable laser source was used to sweep the wavelength and to observe the bottle WGM resonances. From the images the microbottle dimensions were estimated as  $D_s=125\mu\text{m}$ ,  $D_b=185\mu\text{m}$  and  $L_b=400\mu\text{m}$  (Fig. 1(a)).

The fiber taper was coupled to the bottle resonator at various positions starting from the centre of the bottle to the bottle-neck (furthest turning point) and beyond on both sides. Images of tapered fiber excitation with optical coupling at various positions along the bottle are given in Figures 1 (b-h). The difference in modal intensity distributions for different excitation positions is readily observed from scattering. The images in Fig. 1(d-f) clearly show the excitation of bottle modes with characteristic intensity maxima on both sides of the bottle in the vicinity of the corresponding turning points, in close qualitative agreement with theoretical predictions [8,9]. In contrast, the image in Fig. 1(b) shows the predominant excitation of more conventional quasi-equatorial WGMs

similar to those of a highly deformed sphere (spheroid). It is important to note that excitation of the bottle modes from either side of the bottle produced near-identical scattering intensity patterns with lobes on both sides of the bottle as shown in Fig. 1(e) and 1(h). The scattered intensity of the bottle modes (Fig. 1(b-h)) should be contrasted with that of the normal stripped fiber (Fig. 1(i)), which shows no axial confinement.



**Figure 1:** (a) Bottle microresonator, (b-h) bottle resonator when the light was coupled through the tapered fiber at various positions along the length, (i) tapered fiber coupling to a normal stripped fiber with a cladding diameter of about 125  $\mu\text{m}$ .



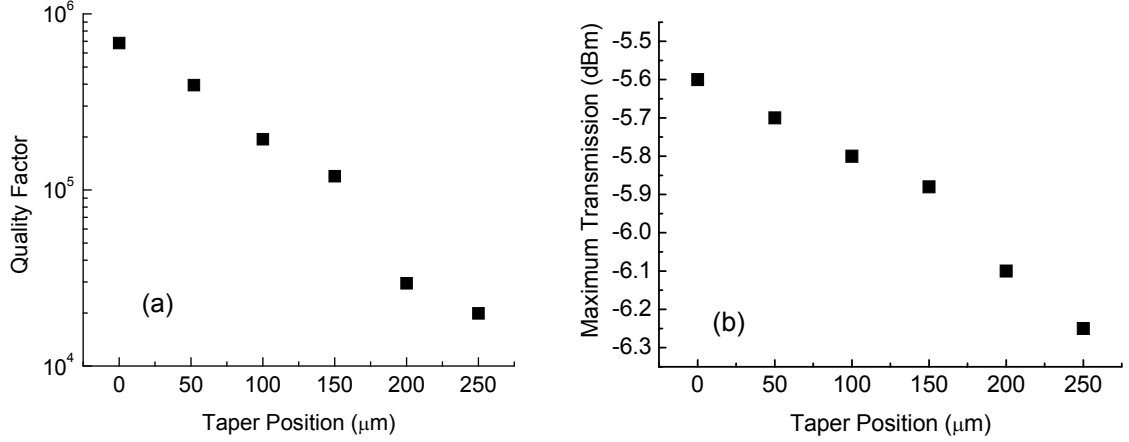
**Figure 2:** (a-f) The resonance spectra for the bottle resonator excited using the tapered fiber at the positions shown in Fig 1. (g) The resonance spectrum for a normal stripped fiber with a diameter of 125  $\mu\text{m}$  excited by a tapered fiber normal to it.

Figure 2 (a)-(f) shows the resonance spectra of the bottle microresonator when excited at various positions along the bottle. For a given bottle shape, the bottle WGMs (b-WGMs) are uniquely defined by three mode numbers  $m$  (azimuthal),  $p$  (radial) and  $q$  (axial) [8,9] and a corresponding characteristic wavelength  $\lambda_{mpq}$ . Due to the strong asphericity of the bottle resonator, all the supported modes are degenerate with strongly overlapping FSRs and very large mode density [10,15]. The wavelength selectivity and the strength of evanescent excitation of the resonator will depend upon the degree of phase-matching and spatial overlap between the tapered-fiber field and the resonator mode fields at the different positions of the tapered fiber. When the fiber taper is placed near the center of the bottle all the b-WGMs are accessible and can be potentially excited. However, only modes with low  $q$  (and large  $m$ ), corresponding to a relatively small separation between turning points, are significantly excited (Fig. 1(b&c)). Modes with very large  $q$ - number show very rapid oscillation of fields around the center of the bottle in the axial direction [9] and therefore are not excited as the field overlap averages to zero. The breaking of degeneracy due to ellipticity results in very dense spectra similar to deformed microspheres [10,15]. The apparent differences in modal density shown in the transmission spectra as the tapered fiber is moved from the bottle centre to the neck is primarily due to differences in modal excitation and selectivity and not inherent modal density changes.

The Q-factors as a function of excitation position are plotted in Figure 3(a) and shown to decrease from  $7 \times 10^5$  to  $2 \times 10^4$  when the tapered fibre excitation moved from the centre of the bottle to 250  $\mu\text{m}$  away from the centre, well beyond the edge of the microbottle. The Q factor of the resonances obtained with the bare normal fiber is about  $1.9 \times 10^4$ . It is shown that the formation of the bottle microresonator results in a more than one order of magnitude, more precisely a factor of 35, increase of the Q factor compared with the corresponding cylindrical resonator (i.e. bare fiber).

During the wavelength characterization, it was observed that the maximum transmitted power level was varied with the fiber taper position (not discernible in Figure 2). In Figure 3(b), we plot the variation of the average maximum transmission, corresponding to wavelengths between resonances (see Figure 2) as a function of the position of the fiber taper. Comparing Figure 3(a) and (b), it is observed that the Q factor variation shows the same functional relation with the transmission loss. The increased losses, as the fibre taper is moved along

the bottle length, are believed to be due to enhanced leakage into air, as well as, into the fibre stems in close proximity to the bottle necks. It should also be noted that there is a marked difference in the variation of both the measured Q factors and the maximum transmission power as the tapered fiber crosses the 200µm point and moves from the outside to well inside the bottle resonator.



**Figure 3:** (a) Q-factors and (b) average maximum transmission as a function of the fiber taper position.

### 3. THEORETICAL RESULTS

To gain further physical insight into the experimental results, the shape of the bottle microresonator under study was fitted with various shape functions, such as harmonic oscillator, parabolic and cosine profiles. The best fitting function for the outer fiber diameter was found to be the truncated harmonic oscillator profile, namely:

$D(z) = D_b [1 + (\Delta k z)^2]^{-1/2}$  for  $|z| \leq L_b/2$  and  $D(z) = D_s$  for  $|z| > L_b/2$  with  $D_b = 185\mu\text{m}$ ,  $D_s = 125\mu\text{m}$  and  $\Delta k = 0.00545 \mu\text{m}^{-1}$ , as shown in Figure 4(a). In this case the allowed modal eigenvalues and axial field distributions are given by well known analytical expressions<sup>11,12</sup>. It can be easily shown that the resonant wavelengths and corresponding turning points can be expressed as

$$\lambda_{mq} = 2\pi m_0 \left[ \left( \frac{m}{R_b} \right)^2 + \left( q + \frac{1}{2} \right) \Delta E_m \right]^{-1/2} \quad (1) \quad \text{and} \quad z_c = \left[ \left( q + \frac{1}{2} \right) 4 / \Delta E_m \right]^{1/2} \quad (2)$$

respectively, as a function of the mode numbers  $m$  and  $q$ , where  $\Delta E_m = 2m\Delta k/R_b$  and  $p=1$  ( $R_b = D_b/2$ ). The microbottle resonator, in addition to a radial potential (similar to microsphere resonators)<sup>20,21</sup>, is characterized by an axial potential given by<sup>11,12</sup>  $V(z) = (m/R(z))^2 - (m/R_b)^2$ . In the case of harmonic oscillator it takes the form  $V(z) = (\Delta E_m z/2)^2$  where  $R(z) = (D(z)/2)$ , while the total energy is given by  $E_{mpq} = k_{mpq}^2 - (m/R_b)^2 = (q+1/2)\Delta E_m$ .

For  $p=1$  and effective turning point of about 50µm, from Equations (1) and (2) it can be deduced that the corresponding b-WGMs are characterized by  $q$  and  $m$  mode-numbers around 40 and 535, respectively, with resonant wavelengths in the 1550nm spectral range. On the other hand, when the fiber taper is moved towards the bottle neck (Fig.1 (d-f,h)), a different sub-set of b-WGMs, with high  $q$ -number, relatively low  $m$ -number, and widely separated turning points are preferentially excited. For turning points around 20µm, 50µm, 250 µm and 200µm, the corresponding  $(m,q)$  pairs are (550,6), (535,40), (430,285) and (375,440), respectively. Group of b-WGMs with mode numbers in the vicinity of the ones reported above show pronounced field maxima around the turning point and are, therefore, expected to overlap strongly with the excitation tapered-fiber beam. Of course, the degree of excitation will also depend critically on the phase-matching conditions.

Figure 4(b) shows the potential (solid) and the total energy (dashed) of the b-WGMs corresponding to turning points 50µm (red), 150µm (green) and 200µm (blue). It is shown that as the turning point moves closer to the bottle neck, the potential becomes shallower, due to the  $m$ -number decrease, while the total energy increases, primarily due to the  $q$ -number increase. As a result, the total mode energy reaches fast the top of the bottle axial potential and, therefore, it becomes easier for modes to leak into the stems in the presence of small surface roughness and other irregularities. It is believed that this leakage effect results in the fast, quasi-exponential decrease of the observed Q factors as the excitation point moved closer to the bottle neck. The quasi-exponential dependence of the Q factor on the mode azimuthal number  $m$  has also been predicted for cylindrical dielectric resonators [17] and microspheres [18].

When the tapered fiber is moved closer to the bottle neck, all the other modes with effective turning points much closer to the bottle center than the current excitation points are not accessible and therefore not excited. This results in seemingly sparser spectra with groups of modes separated by better defined FSR; the groups

excited depend upon fibre taper position and hence taper/WGM overlap. As shown in Fig. 2(c)-(e), the excited modal groups are progressively separated by smaller FSR as the fiber taper moves towards the bottle neck. The FSR observed for the bottle-mode groups in Fig. 2(e) was about 0.4nm near a wavelength of 1550nm, which is about one seventh of the FSR expected for a microsphere with the same diameter ( $\approx 185 \mu\text{m}$ ) as the bottle. This FSR is equivalent to that of a standard FP cavity about five times longer than the bottle length,  $L_b$ . This increased cavity length is due to the long helical path followed by the bottle mode, travelling back and forth between the two turning points close to the bottle necks. When excitation is attempted beyond these points (Fig 2(f)) only the normal fiber WGMs are excited and an FSR of 4.5nm is observed, in agreement with the WGMs expected in the original fiber of cladding diameter  $125 \mu\text{m}$  (Fig. 2(g)).

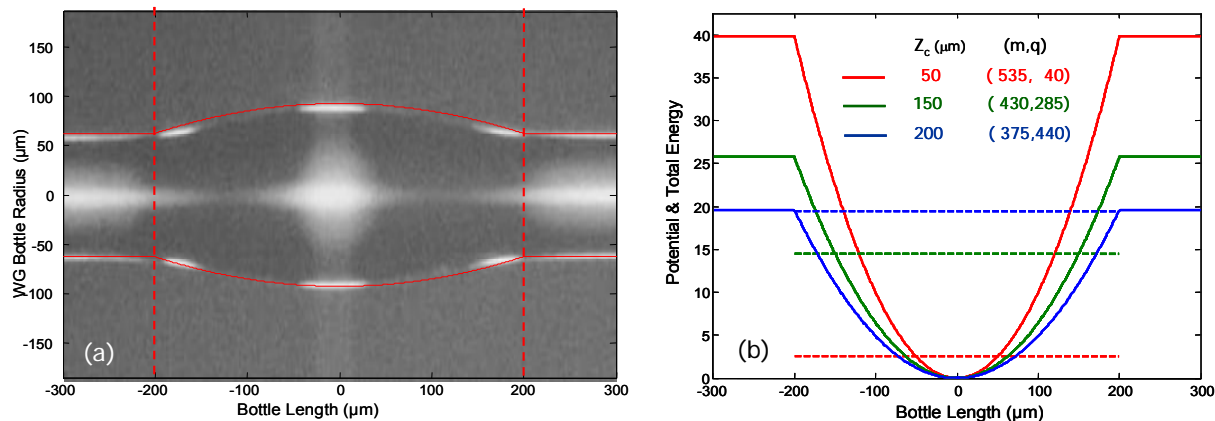


**Figure 4:** (a) Microbottle resonator fitted with truncated harmonic oscillator profile, (b) The potential (solid) and the total energy (dashed) of the b-WGMs corresponding to turning points 50 $\mu\text{m}$  (red), 150 $\mu\text{m}$  (green) and 200 $\mu\text{m}$  (blue).

**4. CONCLUSIONS:** In summary, the existence of bottle modes of high axial order with spatially well-separated intensity maxima at the turning points, a characteristic feature of bottle microresonators, has been experimentally demonstrated for the first time. These modes have been selectively excited using a tapered fiber positioned close to the surface of the bottle. The Q factors of the b-WGMs increased quasi-exponential as the excitation point moved closer to the bottle center. This was shown to be due to the better axial confinement and reduction of the lateral mode leakage. Compared to standard cylindrical resonators, the formation of the bottle microresonator resulted in a 35x improvement of the Q factor, when excited at the bottle waist. The Q factors can be increased further by extra surface treatment, such as chemical or fire polishing, in order to reduce surface roughness and other irregularities.

## ACKNOWLEDGEMENTS

The authors thank Dr. Yongmin Jung for providing the tapered fiber coupler and Dr. Yuh Tat Cho for providing the fusion splicer. This work was funded by the UK EPSRC under grant GR/S96500/01.

## REFERENCES

- [1] B. E. Little, J. S. Foresi, G. Steinmeyer, E. R. Thoen, et al, IEEE Photon. Tech. Lett. **10**, 549 (1998).
- [2] M. Cai, O. Painter, K. J. Vahala and P. C. Sercel, Opt. Lett. **25**, 1430 (2000).
- [3] Chung-Yen Chao and L. Jay Guo, Appl. Phys. Lett. **83**, 1527 (2003).
- [4] F. C. Blom, D. R. van Dijk, H. J. W. M. Hoekstra, A. Driessen, et al, Appl. Phys. Lett. **71**, 747 (1997).
- [5] W. Klitzing, R. Long, V. S. Ilchenko, J. Hare, and V. Lefèvre-Seguin, Opt. Lett. **26**, 166 (2001).
- [6] M. L. Gorodetsky, A. A. Savchenkov, and V. S. Ilchenko, Opt. Lett. **21**, 453 (1996).
- [7] D. K. Armani, T. J. Kippenberg, S. M. Spillane and K. J. Vahala, Nature **421**, 925 (2003).
- [8] M. Sumetsky, Opt. Lett. **29**, 8 (2004).
- [9] Y. Louyer, D. Meshede, and A. Rauschenbeutel, Phys. Rev. A **72**, 031801(R) (2005).
- [10] M. L. Gorodetsky and A. E. Fomin, IEEE J. Selected. Topics. Quant. Elec. **12**, 33 (2006).
- [11] G. Kakarantzas, T. E. Dimmick, T. A. Birks, R. Le Roux and P. St. J. Russell, Opt. Lett., **26**, 1137, (2001).
- [12] J. M. Ward, D. G. O'Shea, B. J. Shortt, M. J. Morrissey, et al, Rev. Sci. Instr., **77**, 083105 (2006).
- [13] F. Warken, A. Rauschenbeutel and T. Bartholomaus, Photonics Spectra **42**, 73 (2008).
- [14] M. N. Zervas, et al, 10<sup>th</sup> Anniv. International Conference on Transparent Optical Networks **4**, 58 (2008).
- [15] G. Chen, Md. M. Mazumder, R. K. Chang, et al Prog. Energy Combust. Sci. **22**, 163 (1996).
- [16] B.R. Johnson, J. Opt. Soc. Am. A, **10**, 343 (1993).
- [17] J.U Nöckel, PhD Thesis, pp. 92-105, Yale University (1997).
- [18] S.M. Lacey, PhD Thesis, pp. 141-147, University of Oregon (2003).